2M4

NASA TECHNICAL NOTE **NASA TN D-7477**

NASA TN D-7477

DERIVATION OF FORMULAS FOR ROOT-MEAN-SQUARE ERRORS IN LOCATION, ORIENTATION, AND SHAPE IN TRIANGULATION SOLUTION OF AN ELONGATED OBJECT IN SPACE

by Sheila Ann T. Long

Langley Research Center
Hampton, Va. 23665

NATIONAL AERONAUTICS AND SPACE ADMINISTRATION • WASHINGTON, D. C. • JUNE 1974

1. Report No.	2. Government Accession No.	3. Recipient's Catalog No.
NASA TN D-7477		

4. Title and Subtitle	5. Report Date
DERIVATION OF FORMULAS FOR ROOT-MEAN-SQUARE ERRORS IN LOCATION, ORIENTATION, AND SHAPE IN TRIANGULATION SOLUTION OF AN ELONGATED OBJECT IN SPACE	June 1974
	6. Performing Organization Code
7. Author(s)	8. Performing Organization Report No.
Sheila Ann T. Long	L-9193
	10. Work Unit No.
9. Performing Organization Name and Address	879-11-36-01
NASA Langley Research Center Hampton, Va. 23665	11. Contract or Grant No.
	13. Type of Report and Period Covered
12. Sponsoring Agency Name and Address	Technical Note
National Aeronautics and Space Administration Washington, D. C. 20546	14. Sponsoring Agency Code

15. Supplementary Notes

16. Abstract

Formulas are derived for the root-mean-square (rms) displacement, slope, and curvature errors in an azimuth-elevation image trace of an elongated object in space, as functions of the number and spacing of the input data points and the rms elevation error in the individual input data points from a single observation station. Also, formulas are derived for the total rms displacement, slope, and curvature error vectors in the triangulation solution of an elongated object in space due to the rms displacement, slope, and curvature errors, respectively, in the azimuth-elevation image traces from different observation stations.

The total rms displacement, slope, and curvature error vectors provide useful measure numbers for determining the relative merits of two or more different triangulation procedures applicable to elongated objects in space. They also provide useful measure numbers for determining the effect of various experimental parameters – such as the number and relative location of the observation stations, the spacing of the input data points along the azimuth-elevation image traces, etc. – on the triangulation solution of an elongated object in space.

17. Key Words (Suggested by Author(s))

Photogrammetry
Ionization trails

18. Distribution Statement

Unclassified – Unlimited

STAR Category 30

19. Security Classif. (of this report)	20. Security Classif. (of this page)	21. No. of Pages	22. Price*
Unclassified	Unclassified	38	$3.25

*For sale by the National Technical Information Service, Springfield, Virginia 22151

DERIVATION OF FORMULAS FOR ROOT-MEAN-SQUARE ERRORS IN LOCATION, ORIENTATION, AND SHAPE IN TRIANGULATION SOLUTION OF AN ELONGATED OBJECT IN SPACE

By Sheila Ann T. Long
Langley Research Center

SUMMARY

Formulas are derived for the root-mean-square (rms) displacement, slope, and curvature errors in an azimuth-elevation image trace of an elongated object in space, as functions of the number and spacing of the input data points and the rms elevation error in the individual input data points from a single observation station. Also, formulas are derived for the total rms displacement, slope, and curvature error vectors in the triangulation solution of an elongated object in space due to the rms displacement, slope, and curvature errors, respectively, in the azimuth-elevation image traces from different observation stations.

INTRODUCTION

The purpose of this paper is to relate the errors in location, orientation, and shape in the triangulation solution of an elongated object in space to the rms elevation errors in the individual input data points. An elongated object, in this paper, is defined as an entity whose lateral dimensions are so small in comparison to its length that it can be regarded as a curved line. One example of such an entity in space is an ionization trail resulting from an object entering the upper atmosphere. A second example is an ionized cloud released in space, such as the barium ion cloud released in the magnetosphere on September 21, 1971 (ref. 1).

In reference 2 a formula is derived for the total distance (i.e., displacement) error vector, which specifies the error in location, in the triangulation solution of a smoke trail in space. For curved lines in space, however, one also needs to specify the errors in orientation and shape. For these, formulas are needed for the total slope and curvature error vectors, respectively. In this paper the total rms slope and curvature, as well as displacement, error vectors are determined.

This paper is composed of two main parts. In the first part a smoothed azimuth-elevation image trace through the azimuth-elevation input data points from a single

observation station is obtained by a least-squares procedure. (The input data points are taken from photographs of the elongated object in space and are initially in terms of right ascension and declination coordinates. A coordinate transformation is then made from right ascension and declination to azimuth and elevation.) Formulas are derived relating the rms displacement, slope, and curvature errors in this smoothed azimuth-elevation image trace to the rms elevation error in the individual input data points.

In the second part of this paper, the errors in the triangulation solution of an elongated object in space are considered. These errors are manifestations of triangulating on azimuth-elevation image traces (and, consequently, input data points) from several observation stations that contain errors. If the input displacement, slope, and curvature errors in the azimuth-elevation image traces are assumed to be small, then one can assume that they give rise to the total rms displacement, slope, and curvature error vectors, respectively, in the triangulation solution. Formulas are derived relating the total rms displacement, slope, and curvature error vectors in the triangulation solution of an elongated object in space to the rms displacement, slope, and curvature errors, respectively, in the azimuth-elevation image traces.

The total rms displacement, slope, and curvature error vectors are useful for determining the relative merits of two or more different triangulation procedures applicable to elongated objects in space. They are also useful for determining the effect of various experimental parameters – such as the number and relative location of the observation stations, the spacing of the input data points along the azimuth-elevation image traces, etc. – on the triangulation solution of an elongated object in space.

SYMBOLS

$A_N^\mu, B_N^\mu, C_N^\mu$ coefficients of second-degree curve $(n-1)^\mu$, n^μ, $(n+1)^\mu$

$a_N^\mu, b_N^\mu, c_N^\mu$ random curvature, slope, and displacement errors in segment $(n-1)^\mu$, n^μ, $(n+1)^\mu$

$d_N^\mu, d_{\lambda N}^\mu, d_{\rho N}^\mu, d_{\phi N}^\mu$ total, east-west, radial, and north-south output displacement errors in solution curve at point N, due to error e_N^μ

$d\nu_N^\mu$ displacement error in curve $(n-1)^\mu$, n^μ, $(n+1)^\mu$ at $v_n^\mu = 0$

$\vec{d}_N^\mu$ total output displacement error vector in solution curve at point N, due to error e_N^μ

e_N^μ input displacement error in segment $(n-1)^\mu$, n^μ, $(n+1)^\mu$

f_N^μ distance between points $n+1$ and $(n+1)^\mu$ in input slope error determination

g_N^μ distance between points n and n^μ in input curvature error determination

h_{nm}^μ coordinates along ordinate axis (i.e., elevation) of individual input data points

$\hat{i}_\lambda, \hat{i}_\rho, \hat{i}_\phi$ unit vectors centered at point N in directions of increasing east longitude, geocentric radius, and geocentric latitude

j quantity which is directly proportional to number of input data points

m index for sequential labeling of individual input data points

N, N^μ indices for sequential labeling of points along curves S and S^μ

n, n^μ indices for sequential labeling of points along traces s and s^μ

r_N^μ input radius of curvature error in segment $(n-1)^\mu$, n^μ, $(n+1)^\mu$

S, S^μ reference and triangulation solution curves of elongated object in space

s, s^μ azimuth-elevation error-free and image traces from station μ

p total number of input data points

p_2, p_4 quantities depending on number of input data points

$\hat{T}_N^\mu, \hat{T}_{N-1}^\mu$ unit vectors in directions of vectors $\overrightarrow{N^\mu, N+1}$ and $\overrightarrow{N-1, N^\mu}$

$\hat{t}_N, \hat{t}_N^\mu$ unit vectors in directions of vectors $\overrightarrow{N, N+1}$ and $\overrightarrow{N, (N+1)^\mu}$

u_{nm}^μ coordinates along abscissa axis [i.e., azimuth $\times$ cos(elevation)] of individual input data points

v_n^μ, w_n^μ — continuous variables along abscissa [i.e., azimuth × cos(elevation)] and ordinate (i.e., elevation) axes of second-degree curve $(n-1)^\mu$, n^μ, $(n+1)^\mu$

x,y,z — rectangular coordinate system with origin at center of earth, x axis in equatorial plane toward Greenwich meridian, z axis toward north, and y axis to form right-hand orthogonal triad

α_N^μ — input slope error in segment $(n-1)^\mu$, n^μ, $(n+1)^\mu$

$\beta_N^\mu, \beta_{1N}^\mu, \beta_{2N}^\mu$ — total, parallel, and perpendicular slope errors in solution curve at point N, due to error α_N^μ

$(\Delta s)_N^\mu$ — spacing between points n and n+1

δ — spacing between coordinates u_{nm}^μ

ϵ_{nm}^μ — deviations associated with individual input data points

ζ_N^μ — vertical displacement of curve $(n-1)^\mu$, n^μ, $(n+1)^\mu$ at $v_n^\mu = 0$

η_N^μ — curvature of curve $(n-1)^\mu$, n^μ, $(n+1)^\mu$ at $v_n^\mu = 0$

$\Theta_N, \Theta_{1N}, \Theta_{2N}$ — total, parallel, and perpendicular rms curvature errors in solution curve at point N

$\theta_N^\mu, \theta_{1N}^\mu, \theta_{2N}^\mu$ — total, parallel, and perpendicular curvature errors, per unit input curvature error, in solution curve at point N

ι_N^μ — input curvature error in segment $(n-1)^\mu$, n^μ, $(n+1)^\mu$

$\kappa_N^\mu, \kappa_{1N}^\mu, \kappa_{2N}^\mu$ — total, parallel, and perpendicular output curvature errors in solution curve at point N, due to error ι_N^μ

$\overrightarrow{\kappa_N^\mu}$ — total output curvature error vector in solution curve at point N, due to error ι_N^μ

λ_N, λ_N^μ — east longitude of points N and N^μ

μ particular observation station

$\Xi_N, \Xi_{\lambda N}, \Xi_{\rho N}, \Xi_{\phi N}$ total, east-west, radial, and north-south rms displacement errors in solution curve at point N

$\xi^{\mu}_N, \xi^{\mu}_{\lambda N}, \xi^{\mu}_{\rho N}, \xi^{\mu}_{\phi N}$ total, east-west, radial, and north-south displacement errors, per unit input displacement error, in solution curve at point N

ρ_N, ρ^{μ}_N geocentric radius of points N and N^{μ}

σ^{μ}_N rms elevation error in individual input data points

$\sigma^{\mu}_{AN}, \sigma^{\mu}_{BN}, \sigma^{\mu}_{CN}$ rms errors in A^{μ}_N, B^{μ}_N, and C^{μ}_N

$\sigma^{\mu}_{aN}, \sigma^{\mu}_{bN}, \sigma^{\mu}_{cN}$ rms curvature, slope, and displacement errors in segment $(n-1)^{\mu}$, n^{μ}, $(n+1)^{\mu}$

ϕ_N, ϕ^{μ}_N geocentric latitude of points N and N^{μ}

ψ^{μ}_N slope of curve $(n-1)^{\mu}$, n^{μ}, $(n+1)^{\mu}$ at $v^{\mu}_n = 0$

$\Omega_N, \Omega_{1N}, \Omega_{2N}$ total, parallel, and perpendicular rms slope errors in solution curve at point N

$\omega^{\mu}_N, \omega^{\mu}_{1N}, \omega^{\mu}_{2N}$ total, parallel, and perpendicular slope errors, per unit input slope error, in solution curve at point N

ANALYSIS

Relationship Between rms Displacement, Slope, and Curvature Errors in an Azimuth-Elevation Image Trace From a Single Observation Station and rms Elevation Error in Individual Input Data Points

In figure 1 an azimuth-elevation plot from the observation station μ of an image trace s^{μ} and an error-free trace s is shown. An azimuth-elevation image trace approximates the actual photographic image of an elongated object in space. An azimuth-elevation error-free trace is the trace that would result if no errors whatsoever occurred

from the data acquisition system and the data reduction procedure. The image trace segment $(n-1)^{\mu}$, n^{μ}, $(n+1)^{\mu}$ differs from the error-free trace segment n-1, n, n+1 in location (i.e., displacement), orientation (i.e., slope) as defined by the first-order derivative, and shape as defined by the second and higher order derivatives. In this paper the highest order derivative considered will be the second; hence, shape will be defined by the single parameter curvature.

For convenience the azimuth-elevation input data points within the segment are selected so that they are equally-spaced along the [azimuth × cos(elevation)] coordinate axis. The segments are sufficiently small so that they can be accurately described by a second-degree curve. Each second-degree curve is obtained by a least-squares procedure. The segment $(n-1)^{\mu}$, n^{μ}, $(n+1)^{\mu}$, centered about the point n^{μ}, of the azimuth-elevation image trace s^{μ} is one such resulting second-degree curve.

The coordinates u_{nm}^{μ} [i.e., azimuth × cos(elevation)] and h_{nm}^{μ} (i.e., elevation), where $m = -j, -j+1, \ldots, -1, 0, 1, \ldots, j-1, j$, of the individual input data points in the interval which gives rise to the second-degree curve $(n-1)^{\mu}$, n^{μ}, $(n+1)^{\mu}$ are shown in figure 2. The deviations ϵ_{nm}^{μ} associated with these individual input data points are

$$\epsilon_{nm}^{\mu} = A_N^{\mu}\left(u_{nm}^{\mu}\right)^2 + B_N^{\mu}u_{nm}^{\mu} + C_N^{\mu} - h_{nm}^{\mu} \tag{1}$$

The coefficients A_N^{μ}, B_N^{μ}, and C_N^{μ} are to be determined. The sum of the squares of the deviations is

$$\sum_{m=-j}^{j}\left(\epsilon_{nm}^{\mu}\right)^2 = \sum_{m=-j}^{j}\left[A_N^{\mu}\left(u_{nm}^{\mu}\right)^2 + B_N^{\mu}u_{nm}^{\mu} + C_N^{\mu} - h_{nm}^{\mu}\right]^2 \tag{2}$$

The following is a generalization of the procedure set forth in reference 3 for the best fit of a straight line to experimental data. In this analysis the best fit of a second-degree curve to the data of interest is the one which minimizes $\sum_{m=-j}^{j}\left(\epsilon_{nm}^{\mu}\right)^2$. Taking the first partial derivatives of equation (2) with respect to A_N^{μ}, B_N^{μ}, and C_N^{μ}, respectively, and then setting each of these three resulting expressions equal to zero, one arrives at

$$A_N^{\mu}\sum_{m=-j}^{j}\left(u_{nm}^{\mu}\right)^4 + B_N^{\mu}\sum_{m=-j}^{j}\left(u_{nm}^{\mu}\right)^3 + C_N^{\mu}\sum_{m=-j}^{j}\left(u_{nm}^{\mu}\right)^2 - \sum_{m=-j}^{j}h_{nm}^{\mu}\left(u_{nm}^{\mu}\right)^2 = 0 \tag{3}$$

$$A_N^{\mu} \sum_{m=-j}^{j} \left(u_{nm}^{\mu}\right)^3 + B_N^{\mu} \sum_{m=-j}^{j} \left(u_{nm}^{\mu}\right)^2 + C_N^{\mu} \sum_{m=-j}^{j} u_{nm}^{\mu} - \sum_{m=-j}^{j} h_{nm}^{\mu} u_{nm}^{\mu} = 0 \tag{4}$$

$$A_N^{\mu} \sum_{m=-j}^{j} \left(u_{nm}^{\mu}\right)^2 + B_N^{\mu} \sum_{m=-j}^{j} u_{nm}^{\mu} + pC_N^{\mu} - \sum_{m=-j}^{j} h_{nm}^{\mu} = 0 \tag{5}$$

The quantity p is the total number of input data points in the interval of interest.

$$p = 2j + 1 \tag{6}$$

Without loss of generality the $2j + 1$ equally-spaced coordinates u_{nm}^{μ} can be centered on a local coordinate origin $\left(\text{i.e., } u_{n0}^{\mu} = 0\right)$. Then,

$$\sum_{m=-j}^{j} u_{nm}^{\mu} = 0 \tag{7}$$

$$\sum_{m=-j}^{j} \left(u_{nm}^{\mu}\right)^2 = p_2 \delta^2 \tag{8}$$

$$\sum_{m=-j}^{j} \left(u_{nm}^{\mu}\right)^3 = 0 \tag{9}$$

$$\sum_{m=-j}^{j} \left(u_{nm}^{\mu}\right)^4 = p_4 \delta^2 \tag{10}$$

The quantity δ is the spacing between the coordinates u_{nm}^{μ} of the individual input data points. The quantities p_2 and p_4, which depend on the number of input data points in the interval of interest, are

$$p_2 = 2\left(1^2 + 2^2 + 3^2 + \ldots + j^2\right)$$

$$= \frac{j(j + 1)(2j + 1)}{3} \tag{11}$$

$$p_4 = 2\left(1^4 + 2^4 + 3^4 + \ldots + j^4\right)$$

$$= \frac{j(j+1)(2j+1)\left(3j^2 + 3j - 1\right)}{15} \tag{12}$$

Substituting equations (7) to (10) into equations (3) to (5) where appropriate, one finds that equations (3) to (5), respectively, become

$$p_4\delta^4 A_N^\mu + p_2\delta^2 C_N^\mu = \sum_{m=-j}^{j} h_{nm}^\mu \left(u_{nm}^\mu\right)^2 \tag{13}$$

$$p_2\delta^2 B_N^\mu = \sum_{m=-j}^{j} h_{nm}^\mu u_{nm}^\mu \tag{14}$$

$$p_2\delta^2 A_N^\mu + pC_N^\mu = \sum_{m=-j}^{j} h_{nm}^\mu \tag{15}$$

after rearranging. Solving the three simultaneous equations (13), (14), and (15), one obtains the coefficients A_N^μ, B_N^μ, and C_N^μ.

$$A_N^\mu = \frac{\sum_{m=-j}^{j} \left[p\left(u_{nm}^\mu\right)^2 - p_2\delta^2\right] h_{nm}^\mu}{\delta^4\left(pp_4 - p_2^2\right)} \tag{16}$$

$$B_N^\mu = \frac{\sum_{m=-j}^{j} u_{nm}^\mu h_{nm}^\mu}{\delta^2 p_2} \tag{17}$$

$$C_N^\mu = \frac{\sum_{m=-j}^{j} \left[p_4\delta^2 - p_2\left(u_{nm}^\mu\right)^2\right] h_{nm}^\mu}{\delta^2\left(pp_4 - p_2^2\right)} \tag{18}$$

One can assume that the individual input data points are uncorrelated. If the rms error in the individual coordinates h_{nm}^μ is denoted by σ_N^μ, then the rms error σ_{AN}^μ in A_N^μ is obtained from the following:

$$\left(\sigma_{AN}^{\mu}\right)^2 = \frac{\sum_{m=-j}^{j}\left[p\left(u_{nm}^{\mu}\right)^2 - p_2\delta^2\right]^2\left(\sigma_N^{\mu}\right)^2}{\delta^8\left(pp_4 - p_2^2\right)^2}$$

using equation (16)

$$= \frac{\left(\sigma_N^{\mu}\right)^2\left[p^2\left(p_4\delta^4\right) - 2pp_2\delta^2\left(p_2\delta^2\right) + p_2^2\delta^4(p)\right]}{\delta^8\left(pp_4 - p_2^2\right)^2}$$

using equations (10), (8), and (6)

$$= \frac{\left(\sigma_N^{\mu}\right)^2 p}{\delta^4\left(pp_4 - p_2^2\right)}$$

Hence, the rms error σ_{AN}^{μ} in A_N^{μ} is

$$\sigma_{AN}^{\mu} = \frac{\sigma_N^{\mu}}{\delta^2}\left(\frac{p}{pp_4 - p_2^2}\right)^{1/2} \tag{19}$$

Similarly, the rms errors in B_N^{μ} and C_N^{μ}, denoted by σ_{BN}^{μ} and σ_{CN}^{μ}, respectively, are

$$\sigma_{BN}^{\mu} = \frac{\sigma_N^{\mu}}{\delta}\frac{1}{\left(p_2\right)^{1/2}} \tag{20}$$

$$\sigma_{CN}^{\mu} = \sigma_N^{\mu}\left(\frac{p_4}{pp_4 - p_2^2}\right)^{1/2} \tag{21}$$

From equations (19), (20), and (21), using equations (6), (11), and (12), one notes that, for large j,

σ_{AN}^{μ} varies approximately as $\left(\frac{1}{\delta j}\right)^2 \frac{1}{(j)^{1/2}}$

σ^{μ}_{BN} varies approximately as $\left(\frac{1}{\delta j}\right)\frac{1}{(j)^{1/2}}$

σ^{μ}_{CN} varies approximately as $\frac{1}{(j)^{1/2}}$

The quantity δ is the spacing between the coordinates u^{μ}_{nm} of the individual input data points, and the quantity j is directly proportional to the number of input data points in the interval of interest.

The equation for the second-degree curve $(n-1)^{\mu}$, n^{μ}, $(n+1)^{\mu}$, centered about the point n^{μ}, is

$$w^{\mu}_{n} = A^{\mu}_{N}\left(v^{\mu}_{n}\right)^{2} + B^{\mu}_{N}v^{\mu}_{n} + C^{\mu}_{N} \tag{22}$$

where v^{μ}_{n} and w^{μ}_{n}, shown in figure 2, are the continuous variables along the abscissa [i.e., azimuth $\times$ cos(elevation)] and ordinate (i.e., elevation) axes, respectively. The vertical displacement ζ^{μ}_{N} of this curve, at $v^{\mu}_{n} = 0$ (i.e., at the point n^{μ}), is

$$\zeta^{\mu}_{N} = w^{\mu}_{n}\Big|_{v^{\mu}_{n}=0}$$

$$= C^{\mu}_{N}$$

The vertical displacement error $d\zeta^{\mu}_{N}$ is

$$d\zeta^{\mu}_{N} = dC^{\mu}_{N}$$

The normal displacement error $d\nu^{\mu}_{N}$ in the curve $(n-1)^{\mu}$, n^{μ}, $(n+1)^{\mu}$, at $v^{\mu}_{n} = 0$, is

$$d\nu^{\mu}_{N} = d\zeta^{\mu}_{N}\cos\left(\tan^{-1}\frac{dw^{\mu}_{n}}{dv^{\mu}_{n}}\right)\Bigg|_{v^{\mu}_{n}=0}$$

$$= dC^{\mu}_{N}\cos\left(\tan^{-1}B^{\mu}_{N}\right)$$

$$= \frac{dC^{\mu}_{N}}{\left[1 + \left(B^{\mu}_{N}\right)^{2}\right]^{1/2}}$$

Therefore, the rms displacement error σ^{μ}_{cN} in the azimuth-elevation image trace segment $(n-1)^{\mu}$, n^{μ}, $(n+1)^{\mu}$, as related to the rms elevation error σ^{μ}_{N} in the individual input data points in the interval of interest, is

$$\sigma^{\mu}_{cN} = \frac{\sigma^{\mu}_{CN}}{\left[1 + \left(B^{\mu}_{N}\right)^2\right]^{1/2}} \tag{23}$$

where σ^{μ}_{CN} is given by equation (21).

The slope ψ^{μ}_{N} of the second-degree curve $(n-1)^{\mu}$, n^{μ}, $(n+1)^{\mu}$, at $v^{\mu}_{n} = 0$, is

$$\psi^{\mu}_{N} = \tan^{-1} \left.\frac{dw^{\mu}_{n}}{dv^{\mu}_{n}}\right|_{v^{\mu}_{n}=0}$$

$$= \tan^{-1} B^{\mu}_{N}$$

The slope error $d\psi^{\mu}_{N}$ is

$$d\psi^{\mu}_{N} = \frac{dB^{\mu}_{N}}{1 + \left(B^{\mu}_{N}\right)^2}$$

Therefore, the rms slope error σ^{μ}_{bN} in the azimuth-elevation image trace segment $(n-1)^{\mu}$, n^{μ}, $(n+1)^{\mu}$, as related to the rms elevation error σ^{μ}_{N} in the individual input data points in the interval of interest, is

$$\sigma^{\mu}_{bN} = \frac{\sigma^{\mu}_{BN}}{1 + \left(B^{\mu}_{N}\right)^2} \tag{24}$$

where σ^{μ}_{BN} is given by equation (20).

The curvature η^{μ}_{N} of the second-degree curve $(n-1)^{\mu}$, n^{μ}, $(n+1)^{\mu}$, at $v^{\mu}_{n} = 0$, is

$$\eta_N^\mu = \left. \frac{\dfrac{d^2 w_n^\mu}{d\left(v_n^\mu\right)^2}}{\left[1 + \left(\dfrac{dw_n^\mu}{dv_n^\mu}\right)^2\right]^{3/2}} \right|_{v_n^\mu = 0}$$

$$= \frac{2A_N^\mu}{\left[1 + \left(B_N^\mu\right)^2\right]^{3/2}}$$

The slope error $d\eta_N^\mu$ is

$$d\eta_N^\mu = \frac{\partial}{\partial A_N^\mu}\left\{\frac{2A_N^\mu}{\left[1 + \left(B_N^\mu\right)^2\right]^{3/2}}\right\} dA_N^\mu + \frac{\partial}{\partial B_N^\mu}\left\{\frac{2A_N^\mu}{\left[1 + \left(B_N^\mu\right)^2\right]^{3/2}}\right\} dB_N^\mu$$

$$= \frac{2dA_N^\mu}{\left[1 + \left(B_N^\mu\right)^2\right]^{3/2}} - \frac{6A_N^\mu B_N^\mu dB_N^\mu}{\left[1 + \left(B_N^\mu\right)^2\right]^{5/2}}$$

Therefore, the rms curvature error σ_{aN}^μ in the azimuth-elevation image trace segment $(n-1)^\mu$, n^μ, $(n+1)^\mu$, as related to the rms elevation error σ_N^μ in the individual input data points in the interval of interest, is

$$\sigma_{aN}^\mu = \left\{\frac{4\left(\sigma_{AN}^\mu\right)^2}{\left[1 + \left(B_N^\mu\right)^2\right]^3} + \frac{36\left(A_N^\mu\right)^2\left(B_N^\mu\right)^2\left(\sigma_{BN}^\mu\right)^2}{\left[1 + \left(B_N^\mu\right)^2\right]^5}\right\}^{1/2} \tag{25}$$

where σ_{AN}^μ and σ_{BN}^μ are given by equations (19) and (20), respectively.

Relationship Between rms Displacement, Slope, and Curvature Errors in the Triangulation Solution of an Elongated Object in Space and rms Displacement, Slope, and Curvature Errors, Respectively, in Azimuth-Elevation Image Traces

Separation of errors.- The output displacement, slope, and curvature errors in the triangulation solution of an elongated object in space are assumed to be small and linearly related to the input displacement, slope, and curvature errors, respectively, in the azimuth-elevation image traces. A linear error analysis model will be derived using perturbations of triangulation solutions to establish the required linear relationships.

The problem reduces to defining the deviation of one curved line in space from a second curved line in its immediate neighborhood. The first curved line is called the reference curve and is denoted by S. The reference curve S, shown in figure 3, is assumed to have the same position and form as the elongated object in space of interest. The points along the curve S are sequentially labeled ..., N-1, N, N+1, ... The geocentric latitude, east longitude, and geocentric radius of the point N on the curve S are denoted by ϕ_N, λ_N, and ρ_N, respectively. In computations one should space the points along the curve S at small, equal intervals in geocentric latitude, east longitude, or geocentric radius, depending on the position and form of the elongated object in space of interest. Also, the points along the curve S should be spaced so that the distances between the successive points are small compared to the geocentric radii of the points. Hence, the arc segments between the successive points along the curve S can be regarded as straight-line segments.

From the curve S, one can derive the azimuth-elevation error-free trace from each of the observation stations of interest. The azimuth-elevation error-free trace s from the observation station μ is shown in figure 4. The points n-1, n, and n+1 along the trace s correspond to the points N-1, N, and N+1, respectively, along the curve S.

The input displacement, slope, and curvature errors are assumed to be small. Hence, one can assume that they give rise to the total rms displacement, slope, and curvature error vectors, respectively. In other words, the total rms displacement, slope, and curvature error vectors are assumed to be effectively decoupled and, consequently, can be examined separately.

One notes that configurations of one, two, and three points define zero, first, and second order derivatives, respectively, if the derivatives are expressed in finite difference notation. This fact will be used in this part of the analysis. In other words, configurations of one, two, and three points will be used in the determinations of the total rms displacement, slope, and curvature error vectors, respectively.

The general procedure for determining the total rms displacement error vector, for instance, will be as follows: Introduce an input displacement error into the error-free trace s from station μ to form an image trace s^{μ}; triangulate, using the trace s^{μ} from station μ and the error-free traces from the remaining stations, to obtain a triangulation solution curve S^{μ}; compare the curve S^{μ} to the curve S to find the total output displacement error vector due to the input displacement error introduced at the station μ; take the ratio of the output to the input displacement errors; and compute the rms sum of this ratio over all of the stations. Analogous procedures will also be carried out with regard to the total rms slope and curvature error vectors.

Displacement errors.- The determination of the total rms displacement error vector will be considered first. For this the points $n-1$, n, and $n+1$ on the azimuth-elevation error-free trace s from the observation station μ are displaced through e_N^{μ} radians along the normals to the trace s at the points $n-1$, n, and $n+1$, respectively, to form the points $(n-1)^{\mu}$, n^{μ}, and $(n+1)^{\mu}$, respectively, as shown in figure 4. The segment $(n-1)^{\mu}$, n^{μ}, $(n+1)^{\mu}$, extended, is the azimuth-elevation image trace s^{μ} from the observation station μ. The quantity e_N^{μ} is the input displacement error in the azimuth-elevation image trace segment $(n-1)^{\mu}$, n^{μ}, $(n+1)^{\mu}$ from the observation station μ.

The triangulation solution of the elongated object in space is then calculated, using for input data the points along the azimuth-elevation image trace s^{μ} from the observation station μ in conjunction with the points along the azimuth-elevation error-free traces from all of the remaining observation stations. Three appropriate triangulation procedures for a curved line in space are described in references 4, 5, and 6.

The resulting triangulation solution curve of the elongated object in space is denoted by S^{μ} and is shown in figure 3. The points along the curve S^{μ} are spaced according to the same scheme as that used for spacing the points along the curve S. They are spaced at the same small, equal intervals in geocentric latitude, east longitude, or geocentric radius that were used for the spacing of the points along the curve S. The point on the curve S^{μ} which has the same geocentric latitude, east longitude, or geocentric radius as the point N on the curve S is denoted by N^{μ}. The geocentric latitude, east longitude, and geocentric radius of the point N^{μ} are denoted by ϕ_N^{μ}, λ_N^{μ}, and ρ_N^{μ}, respectively. (One should notice that no correspondence exists between the points N^{μ} and n^{μ}, unlike the situation for the points N and n.)

The vector $\overrightarrow{N,N+1}$, from the point N to the point $N+1$, shown in figure 3, is

$$\begin{aligned}\overrightarrow{N,N+1} &= \rho_{N+1} \cos \phi_{N+1} \sin\left(\lambda_{N+1} - \lambda_N\right)\hat{i}_\lambda \\ &+ \rho_{N+1}\left[\sin \phi_{N+1} \cos \phi_N - \cos \phi_{N+1} \sin \phi_N \cos\left(\lambda_{N+1} - \lambda_N\right)\right]\hat{i}_\phi \\ &+ \left\{\rho_{N+1}\left[\cos \phi_{N+1} \cos \phi_N \cos\left(\lambda_{N+1} - \lambda_N\right) + \sin \phi_{N+1} \sin \phi_N\right] - \rho_N\right\}\hat{i}_\rho \end{aligned} \quad (26)$$

where $\hat{i}_\lambda$, $\hat{i}_\phi$, and $\hat{i}_\rho$ are the unit vectors centered at the point N in the directions of increasing east longitude, geocentric latitude, and geocentric radius, respectively, where ϕ_N, λ_N, and ρ_N are the geocentric latitude, east longitude, and geocentric radius, respectively, of the point N, and where ϕ_{N+1}, λ_{N+1}, and ρ_{N+1} are the geocentric latitude, east longitude, and geocentric radius, respectively, of the point $N+1$. The unit vector $\hat{t}_N$, shown in figure 3, which is in the same direction as the vector $\overrightarrow{N,N+1}$, is

$$\hat{t}_N = \frac{\overrightarrow{N,N+1}}{\left|\overrightarrow{N,N+1}\right|} \quad (27)$$

The vector $\overrightarrow{N,N^\mu}$, from the point N to the point N^μ, in figure 3, is

$$\begin{aligned}\overrightarrow{N,N^\mu} &= \rho_N^\mu \cos \phi_N^\mu \sin\left(\lambda_N^\mu - \lambda_N\right)\hat{i}_\lambda \\ &+ \rho_N^\mu\left[\sin \phi_N^\mu \cos \phi_N - \cos \phi_N^\mu \sin \phi_N \cos\left(\lambda_N^\mu - \lambda_N\right)\right]\hat{i}_\phi \\ &+ \left\{\rho_N^\mu\left[\cos \phi_N^\mu \cos \phi_N \cos\left(\lambda_N^\mu - \lambda_N\right) + \sin \phi_N^\mu \sin \phi_N\right] - \rho_N\right\}\hat{i}_\rho \end{aligned} \quad (28)$$

where ϕ_N^μ, λ_N^μ, and ρ_N^μ are the geocentric latitude, east longitude, and geocentric radius, respectively, of the point N^μ.

The vector $\overrightarrow{d_N^\mu}$, shown in figure 3, which is drawn from and normal to the curve S, at the point N, to the curve S^μ, very closely approximates the shortest vector distance from the curve S to the point N^μ. The vector $\overrightarrow{d_N^\mu}$ is the total output displacement error vector in the triangulation solution curve at the point N, due to the input displacement error e_N^μ.

From figure 3 one sees that

$$\overrightarrow{d_N^\mu} = \overrightarrow{N,N^\mu} - \left(\overrightarrow{N,N^\mu} \cdot \hat{t}_N\right)\hat{t}_N \tag{29}$$

Substitution of equations (27) and (28) into equation (29) leads to an equation for the vector $\overrightarrow{d_N^\mu}$ in the following form:

$$\overrightarrow{d_N^\mu} = d_{\lambda N}^\mu \hat{i}_\lambda + d_{\phi N}^\mu \hat{i}_\phi + d_{\rho N}^\mu \hat{i}_\rho \tag{30}$$

where $d_{\lambda N}^\mu$, $d_{\phi N}^\mu$, and $d_{\rho N}^\mu$ are the east-west (i.e., in the direction of increasing east longitude), north-south (i.e., in the direction of increasing geocentric latitude), and radial (i.e., in the direction of increasing geocentric radius) output displacement errors in the solution curve at the point N, due to the input displacement error e_N^μ. The total output displacement error d_N^μ in the solution curve at the point N, due to the input displacement error e_N^μ, is

$$d_N^\mu = \left[\left(d_{\lambda N}^\mu\right)^2 + \left(d_{\phi N}^\mu\right)^2 + \left(d_{\rho N}^\mu\right)^2\right]^{1/2} \tag{31}$$

Hence, the east-west, north-south, radial, and total displacement errors, denoted by $\xi_{\lambda N}^\mu$, $\xi_{\phi N}^\mu$, $\xi_{\rho N}^\mu$, and ξ_N^μ, respectively, per unit input displacement error, in the solution curve at the point N are

$$\xi_{\lambda N}^\mu = \frac{d_{\lambda N}^\mu}{e_N^\mu} \tag{32}$$

$$\xi_{\phi N}^\mu = \frac{d_{\phi N}^\mu}{e_N^\mu} \tag{33}$$

$$\xi_{\rho N}^\mu = \frac{d_{\rho N}^\mu}{e_N^\mu} \tag{34}$$

$$\xi_N^\mu = \frac{d_N^\mu}{e_N^\mu} \tag{35}$$

Now, the east-west displacement error $\xi^{\mu}_{\lambda N}$, for instance, in the solution curve at the point N is due only to the unit input displacement error in the azimuth-elevation image trace segment $(n-1)^{\mu}$, n^{μ}, $(n+1)^{\mu}$ from the observation station μ. If a random normal displacement error, c^{μ}_{N}, with zero mean exists in the segment $(n-1)^{\mu}$, n^{μ}, $(n+1)^{\mu}$ from the station μ, then the east-west displacement error in the solution curve at the point N, due to the random displacement error c^{μ}_{N}, is $\left(\xi^{\mu}_{\lambda N}\, c^{\mu}_{N}\right)$. Hence, the east-west rms displacement error $\Xi_{\lambda N}$ in the solution curve at the point N, due to the random displacement error c^{μ}_{N} in the azimuth-elevation image trace segment $(n-1)^{\mu}$, n^{μ}, $(n+1)^{\mu}$ from each of the respective observation stations, is

$$\Xi_{\lambda N} = \left[\overline{\left(\sum_{\mu} \xi^{\mu}_{\lambda N}\, c^{\mu}_{N}\right)^{2}}\right]^{1/2} \tag{36}$$

The bar denotes the mean value, and the summation is over the total number of observation stations. Because the random displacement errors c^{μ}_{N} at the various observation stations are uncorrelated, equation (36) becomes

$$\Xi_{\lambda N} = \left[\sum_{\mu} \left(\xi^{\mu}_{\lambda N}\right)^{2} \overline{\left(c^{\mu}_{N}\right)^{2}}\right]^{1/2} \tag{37}$$

If one assumes that the mean-square random displacement error $\overline{\left(c^{\mu}_{N}\right)^{2}}$ in the azimuth-elevation image trace segment $(n-1)^{\mu}$, n^{μ}, $(n+1)^{\mu}$ from each respective observation station is equal to $\left(\sigma^{\mu}_{cN}\right)^{2}$ radians [the mean-square displacement error in the azimuth-elevation image trace segment $(n-1)^{\mu}$, n^{μ}, $(n+1)^{\mu}$ as given by equation (23)], then equation (37) becomes

$$\Xi_{\lambda N} = \left[\sum_{\mu} \left(\xi^{\mu}_{\lambda N}\right)^{2} \left(\sigma^{\mu}_{cN}\right)^{2}\right]^{1/2} \tag{38}$$

Therefore, equation (38) is the formula for the east-west rms displacement error in the triangulation solution curve at the point N, as related to the rms displacement errors σ^{μ}_{cN} in the azimuth-elevation image traces. Similarly, the north-south, radial, and total rms displacement errors, denoted by $\Xi_{\phi N}$, $\Xi_{\rho N}$, and Ξ_{N}, respectively, in the triangulation solution curve at the point N, as related to the rms displacement errors σ^{μ}_{cN} in the azimuth-elevation image traces, are

$$\Xi_{\phi N} = \left[\sum_{\mu} \left(\xi^{\mu}_{\phi N} \right)^2 \left(\sigma^{\mu}_{cN} \right)^2 \right]^{1/2} \tag{39}$$

$$\Xi_{\rho N} = \left[\sum_{\mu} \left(\xi^{\mu}_{\rho N} \right)^2 \left(\sigma^{\mu}_{cN} \right)^2 \right]^{1/2} \tag{40}$$

$$\Xi_{N} = \left[\sum_{\mu} \left(\xi^{\mu}_{N} \right)^2 \left(\sigma^{\mu}_{cN} \right)^2 \right]^{1/2} \tag{41}$$

Slope errors.- In this section the relationship between the total rms slope error vector in the triangulation solution of an elongated object in space and the rms slope errors in the azimuth-elevation image traces is considered. For this determination a triangulation solution of the elongated object in space is calculated, using for input data the points along the azimuth-elevation image trace segment n, $(n+1)^{\mu}$, extended, denoted by s^{μ}, and shown in figure 5, from the observation station μ in conjunction with the points along the azimuth-elevation error-free traces from all of the remaining observation stations. One notes that the segment n, $(n+1)^{\mu}$ has one extremity on the trace s. This is permissible, without loss of generality, because the total rms slope error vector has been assumed to be effectively decoupled from the total rms displacement error vector. (The point $(n+1)^{\mu}$ in fig. 5 is not necessarily the same as the point $(n+1)^{\mu}$ in fig. 4.) The resulting triangulation solution curve S^{μ} of the elongated object in space extends through the segment N, $(N+1)^{\mu}$, as shown in figure 6. (There is no correspondence between the point $(N+1)^{\mu}$ in fig. 6 and the point $(n+1)^{\mu}$ in fig. 5 and the point $(N+1)^{\mu}$ in fig. 6 is not the same as the point $(N+1)^{\mu}$ in fig. 3.)

The angle α^{μ}_{N}, shown in figure 5, between the segment n, n+1 and the segment n, $(n+1)^{\mu}$ is the input slope error in the azimuth-elevation image trace segment $(n-1)^{\mu}$, n^{μ}, $(n+1)^{\mu}$ from the observation station μ. The angle β^{μ}_{N}, shown in figure 6, between the segment N, N+1 and the segment N, $(N+1)^{\mu}$ is the total output slope error in the triangulation solution curve at the point N, due to the input slope error α^{μ}_{N}. The first step in this section is to determine the equations for the total output slope error β^{μ}_{N} and the input slope error α^{μ}_{N}.

The vector from the point N to the point $(N+1)^{\mu}$, in figure 6, is $\overrightarrow{N,(N+1)^{\mu}}$.

$$\overrightarrow{N,(N+1)^{\mu}} = \rho_{N+1}^{\mu} \cos \phi_{N+1}^{\mu} \sin\left(\lambda_{N+1}^{\mu} - \lambda_N\right)\hat{i}_{\lambda}$$

$$+ \rho_{N+1}^{\mu}\left[\sin \phi_{N+1}^{\mu} \cos \phi_N - \cos \phi_{N+1}^{\mu} \sin \phi_N \cos\left(\lambda_{N+1}^{\mu} - \lambda_N\right)\right]\hat{i}_{\phi}$$

$$+ \left\{\rho_{N+1}^{\mu}\left[\cos \phi_{N+1}^{\mu} \cos \phi_N \cos\left(\lambda_{N+1}^{\mu} - \lambda_N\right) + \sin \phi_{N+1}^{\mu} \sin \phi_N\right] - \rho_N\right\}\hat{i}_{\rho} \tag{42}$$

where ϕ_{N+1}^{μ}, λ_{N+1}^{μ}, and ρ_{N+1}^{μ} are the geocentric latitude, east longitude, and geocentric radius, respectively, of the point $(N+1)^{\mu}$. The unit vector $\hat{t}_N^{\mu}$, shown in figure 6, which is in the same direction as the vector $\overrightarrow{N,(N+1)^{\mu}}$, is

$$\hat{t}_N^{\mu} = \frac{\overrightarrow{N,(N+1)^{\mu}}}{\left|\overrightarrow{N,(N+1)^{\mu}}\right|} \tag{43}$$

Also from figure 6 one sees that the total output slope error β_N^{μ} in the solution curve at the point N, due to the input slope error α_N^{μ}, is

$$\beta_N^{\mu} = \sin^{-1}\left|\hat{t}_N \times \hat{t}_N^{\mu}\right| \tag{44}$$

where the unit vector $\hat{t}_N$ is given by equation (27). Now, the unit vector that is normal to the local vertical tangent plane is $\left(\frac{\hat{t}_N \times \hat{i}_{\rho}}{\left|\hat{t}_N \times \hat{i}_{\rho}\right|}\right)$, which is seen from figure 6. The local vertical tangent plane, here, is the plane passing through the earth's center and tangent to the reference curve S at the point N. The total output slope error β_N^{μ} can be resolved into two components, the parallel output slope error β_{1N}^{μ} (parallel to the local vertical tangent plane) and the perpendicular output slope error β_{2N}^{μ} (perpendicular to the local vertical tangent plane). From figure 6 one observes that, for small slope errors, the perpendicular output slope error β_{2N}^{μ} and the parallel output slope error β_{1N}^{μ} in the solution curve at the point N, due to the input slope error α_N^{μ}, are

$$\beta_{2N}^{\mu} = \left(\hat{t}_N \times \hat{t}_N^{\mu}\right) \cdot \frac{\left(\hat{t}_N \times \hat{i}_\rho\right)}{\left|\hat{t}_N \times \hat{i}_\rho\right|} \tag{45}$$

$$\beta_{1N}^{\mu} = \left[\left(\beta_N^{\mu}\right)^2 - \left(\beta_{2N}^{\mu}\right)^2\right]^{1/2} \tag{46}$$

From figure 5 one sees that the input slope error α_N^{μ} in the azimuth-elevation image trace segment $(n-1)^{\mu}$, n^{μ}, $(n+1)^{\mu}$ from the observation station μ is

$$\alpha_N^{\mu} = \tan^{-1}\left[\frac{f_N^{\mu}}{(\Delta s)_N^{\mu}}\right] \tag{47}$$

The quantity $(\Delta s)_N^{\mu}$ is the spacing in radians between the points n and n+1, and the quantity f_N^{μ} is the distance in radians between the points n+1 and $(n+1)^{\mu}$. (In computations one may set the quantity f_N^{μ} equal to the input displacement error e_N^{μ}.) Hence, the parallel, perpendicular, and total slope errors, denoted by ω_{1N}^{μ}, ω_{2N}^{μ}, and ω_N^{μ}, respectively, per unit input slope error, in the solution curve at the point N are

$$\omega_{1N}^{\mu} = \frac{\beta_{1N}^{\mu}}{\alpha_N^{\mu}} \tag{48}$$

$$\omega_{2N}^{\mu} = \frac{\beta_{2N}^{\mu}}{\alpha_N^{\mu}} \tag{49}$$

$$\omega_N^{\mu} = \frac{\beta_N^{\mu}}{\alpha_N^{\mu}} \tag{50}$$

Now, the parallel slope error ω_{1N}^{μ}, for instance, in the solution curve at the point N is due only to the unit input slope error in the azimuth-elevation image trace segment $(n-1)^{\mu}$, n^{μ}, $(n+1)^{\mu}$ from the observation station μ. If a random slope error b_N^{μ} with zero mean exists in the segment $(n-1)^{\mu}$, n^{μ}, $(n+1)^{\mu}$ from the station μ, then the parallel slope error in the solution curve at the point N, due to the random slope error b_N^{μ}, is $\left(\omega_{1N}^{\mu}\, b_N^{\mu}\right)$. The random slope errors at the various observation stations, like the random displacement errors, are uncorrelated. If one assumes that the

mean-square random slope error $\overline{\left(b_N^{\mu}\right)^2}$ in the azimuth-elevation image trace segment $(n-1)^{\mu}$, n^{μ}, $(n+1)^{\mu}$ from each respective observation station is equal to $\left(\sigma_{bN}^{\mu}\right)^2$ radians (the mean-square slope error in the azimuth-elevation image trace segment $(n-1)^{\mu}$, n^{μ}, $(n+1)^{\mu}$ as given by eq. (24)), then

$$\Omega_{1N} = \left[\sum_{\mu}\left(\omega_{1N}^{\mu}\right)^2\left(\sigma_{bN}^{\mu}\right)^2\right]^{1/2} \tag{51}$$

is the formula for the parallel rms slope error in the triangulation solution curve at the point N, as related to the rms slope errors σ_{bN}^{μ} in the azimuth-elevation image traces. Similarly, the perpendicular and total slope errors, denoted by Ω_{2N} and Ω_N, respectively, in the triangulation solution curve at the point N, as related to the rms slope errors σ_{bN}^{μ} in the azimuth-elevation image traces, are

$$\Omega_{2N} = \left[\sum_{\mu}\left(\omega_{2N}^{\mu}\right)^2\left(\sigma_{bN}^{\mu}\right)^2\right]^{1/2} \tag{52}$$

$$\Omega_{N} = \left[\sum_{\mu}\left(\omega_{N}^{\mu}\right)^2\left(\sigma_{bN}^{\mu}\right)^2\right]^{1/2} \tag{53}$$

Curvature errors.- In this section the relationship between the total rms curvature error vector in the triangulation solution of an elongated object in space and the rms curvature errors in the azimuth-elevation image traces is considered. For this determination a triangulation solution of the elongated object in space is calculated, using for input data the points along the azimuth-elevation image trace segment n-1, n^{μ}, n+1, extended, denoted by s^{μ}, and shown in figure 7, from the observation station μ in conjunction with the points along the azimuth-elevation error-free traces from all of the remaining observation stations. One notes that the segment n-1, n^{μ}, n+1 has both of its extremities on the trace s. This is permissible, without loss of generality, because the total rms curvature error vector has been assumed to be effectively decoupled from both the total rms displacement and slope error vectors. (The point n^{μ} in fig. 7 is not necessarily the same as the point n^{μ} in fig. 4.) The resulting triangulation solution curve S^{μ} of the elongated object in space extends through the segment N-1, N^{μ}, N+1, as shown in figure 8. (No correspondence exists between the point N^{μ} in fig. 8 and the point n^{μ} in fig. 7, and the point N^{μ} in fig. 8 is not the same as the point N^{μ} in fig. 3.)

The input curvature error ι_N^μ (i.e., the reciprocal of the input radius of curvature error r_N^μ) in the azimuth-elevation image trace segment $(n-1)^\mu$, n^μ, $(n+1)^\mu$ from the observation station μ is shown in figure 7. The total output curvature error vector $\overrightarrow{\kappa_N^\mu}$ in the triangulation solution curve at the point N, due to the input curvature error ι_N^μ, is shown in figure 8. The first step in this section is to determine the equations for the total output curvature error vector $\overrightarrow{\kappa_N^\mu}$ and the input curvature error ι_N^μ.

The vector $\overrightarrow{N^\mu,N+1}$, from the point N^μ to the point N+1, in figure 8, is

$$\begin{aligned}\overrightarrow{N^\mu,N+1} = &\left[\rho_{N+1}\cos\phi_{N+1}\sin(\lambda_{N+1}-\lambda_N) - \rho_N^\mu\cos\phi_N^\mu\sin(\lambda_N^\mu-\lambda_N)\right]\hat{i}_\lambda \\ &+\left\{\rho_{N+1}\left[\sin\phi_{N+1}\cos\phi_N - \cos\phi_{N+1}\sin\phi_N\cos(\lambda_{N+1}-\lambda_N)\right]\right. \\ &\left.-\rho_N^\mu\left[\sin\phi_N^\mu\cos\phi_N - \cos\phi_N^\mu\sin\phi_N\cos(\lambda_N^\mu-\lambda_N)\right]\right\}\hat{i}_\phi \\ &+\left\{\rho_{N+1}\left[\sin\phi_{N+1}\sin\phi_N + \cos\phi_{N+1}\cos\phi_N\cos(\lambda_{N+1}-\lambda_N)\right]\right. \\ &\left.-\rho_N^\mu\left[\sin\phi_N^\mu\sin\phi_N + \cos\phi_N^\mu\cos\phi_N\cos(\lambda_N^\mu-\lambda_N)\right]\right\}\hat{i}_\rho \end{aligned} \tag{54}$$

The unit vector $\hat{T}_N^\mu$, shown in figure 8, which is in the same direction as the vector $\overrightarrow{N^\mu,N+1}$, is

$$\hat{T}_N^\mu = \frac{\overrightarrow{N^\mu,N+1}}{\left|\overrightarrow{N^\mu,N+1}\right|} \tag{55}$$

The vector $\overrightarrow{N-1,N^\mu}$, from the point N-1 to the point N^μ, in figure 8, is

$$\overrightarrow{N-1,N^{\mu}} = \left[\rho_N^{\mu} \cos \phi_N^{\mu} \sin\left(\lambda_N^{\mu} - \lambda_N\right) + \rho_{N-1} \cos \phi_{N-1} \sin\left(\lambda_N - \lambda_{N-1}\right)\right] \hat{i}_{\lambda}$$

$$+ \left\{\rho_N^{\mu}\left[\sin \phi_N^{\mu} \cos \phi_N - \cos \phi_N^{\mu} \sin \phi_N \cos\left(\lambda_N^{\mu} - \lambda_N\right)\right]\right.$$

$$\left. - \rho_{N-1}\left[\cos \phi_N \sin \phi_{N-1} - \sin \phi_N \cos \phi_{N-1} \cos\left(\lambda_N - \lambda_{N-1}\right)\right]\right\} \hat{i}_{\phi}$$

$$+ \left\{\rho_N^{\mu}\left[\sin \phi_N^{\mu} \sin \phi_N + \cos \phi_N^{\mu} \cos \phi_N \cos\left(\lambda_N^{\mu} - \lambda_N\right)\right]\right.$$

$$\left. - \rho_{N-1}\left[\sin \phi_N \sin \phi_{N-1} + \cos \phi_N \cos \phi_{N-1} \cos\left(\lambda_N - \lambda_{N-1}\right)\right]\right\} \hat{i}_{\rho} \qquad (56)$$

where ϕ_{N-1}, λ_{N-1}, and ρ_{N-1} are the geocentric latitude, east longitude, and geocentric radius, respectively, of the point N-1. The unit vector $\hat{T}_{N-1}^{\mu}$, shown in figure 8, which is in the same direction as the vector $\overrightarrow{N-1,N^{\mu}}$, is

$$\hat{T}_{N-1}^{\mu} = \frac{\overrightarrow{N-1,N^{\mu}}}{\left|\overrightarrow{N-1,N^{\mu}}\right|} \qquad (57)$$

If the curvature of the reference curve S is small compared to the curvature of the triangulation solution curve S^{μ}, then the total output curvature error vector $\overrightarrow{\kappa_N^{\mu}}$ in the solution curve at the point N, due to the input curvature error ι_N^{μ}, is approximately

$$\overrightarrow{\kappa_N^{\mu}} = \frac{\hat{T}_N^{\mu} - \hat{T}_{N-1}^{\mu}}{\left|\overrightarrow{N-1,N^{\mu}}\right|} \qquad (58)$$

as is seen from figure 8. The total output curvature error κ_N^{μ} in the solution curve at the point N, due to the input curvature error ι_N^{μ}, is

$$\kappa_N^{\mu} = \left|\overrightarrow{\kappa_N^{\mu}}\right| \qquad (59)$$

The total output curvature error can be resolved into two components, the parallel output curvature error κ^{μ}_{1N} (parallel to the local vertical tangent plane, as defined in the previous section on slope errors) and the perpendicular output curvature error κ^{μ}_{2N} (perpendicular to the local vertical tangent plane). The perpendicular output curvature error κ^{μ}_{2N} and the parallel output curvature error κ^{μ}_{1N} in the solution curve at the point N, due to the input curvature error ι^{μ}_{N}, are

$$\kappa^{\mu}_{2N} = \overrightarrow{\kappa^{\mu}_{N}} \cdot \frac{\left(\hat{t}_N \times \hat{i}_\rho\right)}{\left|\hat{t}_N \times \hat{i}_\rho\right|} \tag{60}$$

$$\kappa^{\mu}_{1N} = \left[\left(\kappa^{\mu}_{N}\right)^2 - \left(\kappa^{\mu}_{2N}\right)^2\right]^{1/2} \tag{61}$$

where the unit vector $\hat{t}_N$ is given by equation (27).

Now, the point n^{μ} is approximately midway between the points n-1 and n+1 along the azimuth-elevation image trace segment n-1, n^{μ}, n+1 and also the quantity g^{μ}_{N}, which is the distance in radians between the points n and n^{μ}, is much smaller than the input radius of curvature error r^{μ}_{N}, as are shown in figure 7. Hence, one finds that, to sufficient accuracy, the input radius of curvature error r^{μ}_{N} in the azimuth-elevation image trace segment $(n-1)^{\mu}$, n^{μ}, $(n+1)^{\mu}$ from the observation station μ is

$$r^{\mu}_{N} = \frac{\left[(\Delta s)^{\mu}_{N}\right]^2}{2g^{\mu}_{N}} \tag{62}$$

where $(\Delta s)^{\mu}_{N}$ is the spacing in radians between the points n and n+1.

Hence, the input curvature error ι^{μ}_{N} in the azimuth-elevation image trace segment $(n-1)^{\mu}$, n^{μ}, $(n+1)^{\mu}$ from the observation station μ is

$$\iota^{\mu}_{N} = \frac{2g^{\mu}_{N}}{\left[(\Delta s)^{\mu}_{N}\right]^2} \tag{63}$$

(In computations the quantity g^{μ}_{N} may be set equal to the input displacement error e^{μ}_{N}.) Hence, the parallel, perpendicular, and total curvature errors, denoted by θ^{μ}_{1N}, θ^{μ}_{2N}, and θ^{μ}_{N}, respectively, per unit input curvature error, in the solution curve at the point N are

$$\theta_{1N}^{\mu} = \frac{\kappa_{1N}^{\mu}}{\iota_N^{\mu}} \tag{64}$$

$$\theta_{2N}^{\mu} = \frac{\kappa_{2N}^{\mu}}{\iota_N^{\mu}} \tag{65}$$

$$\theta_N^{\mu} = \frac{\kappa_N^{\mu}}{\iota_N^{\mu}} \tag{66}$$

Now, the parallel curvature error θ_{1N}^{μ}, for instance, in the solution curve at the point N is due only to the unit input curvature error in the azimuth-elevation image trace segment $(n-1)^{\mu}$, n^{μ}, $(n+1)^{\mu}$ from the observation station μ. If a random curvature error a_N^{μ} with zero mean exists in the segment $(n-1)^{\mu}$, n^{μ}, $(n+1)^{\mu}$ from the station μ, then the parallel curvature error in the solution curve at the point N, due to the random curvature error a_N^{μ}, is $\left(\theta_{1N}^{\mu}\, a_N^{\mu}\right)$. The random curvature errors at the various observation stations, like both the random displacement and slope errors, are uncorrelated. If one assumes that the mean-square random curvature error $\overline{\left(a_N^{\mu}\right)^2}$ in the azimuth-elevation image trace segment $(n-1)^{\mu}$, n^{μ}, $(n+1)^{\mu}$ from each respective observation station is equal to $\left(\sigma_{aN}^{\mu}\right)^2$ radians (the mean-square curvature error in the azimuth-elevation image trace segment $(n-1)^{\mu}$, n^{μ}, $(n+1)^{\mu}$ as given by eq. (25)), then

$$\Theta_{1N} = \left[\sum_{\mu}\left(\theta_{1N}^{\mu}\right)^2\left(\sigma_{aN}^{\mu}\right)^2\right]^{1/2} \tag{67}$$

is the formula for the parallel rms curvature error in the triangulation solution curve at the point N, as related to the rms curvature errors σ_{aN}^{μ} in the azimuth-elevation image traces. Similarly, the perpendicular and total rms curvature errors, denoted by Θ_{2N} and Θ_N, respectively, in the triangulation solution curve at the point N, as related to the rms curvature errors σ_{aN}^{μ} in the azimuth-elevation image traces, are

$$\Theta_{2N} = \left[\sum_{\mu}\left(\theta_{2N}^{\mu}\right)^2\left(\sigma_{aN}^{\mu}\right)^2\right]^{1/2} \tag{68}$$

$$\Theta_N = \left[\sum_{\mu} \left(\theta_N^{\mu} \right)^2 \left(\sigma_{aN}^{\mu} \right)^2 \right]^{1/2} \tag{69}$$

CONCLUDING REMARKS

Formulas have been derived for the rms displacement, slope, and curvature errors in an azimuth-elevation image trace of an elongated object in space, as related to the rms elevation error in the individual input data points. Also, formulas have been derived for the total rms displacement, slope, and curvature error vectors in the triangulation solution of an elongated object in space, as related to the rms displacement, slope, and curvature errors, respectively, in the azimuth-elevation image traces. These total rms displacement, slope, and curvature error vectors specify the errors in location, orientation, and shape, respectively, in the triangulation solution of an elongated object in space. Therefore, the errors in location, orientation, and shape in the triangulation solution of an elongated object in space have been related to the rms elevation errors in the individual input data points.

Langley Research Center,
National Aeronautics and Space Administration,
Hampton, Va., January 23, 1974.

REFERENCES

1. Adamson, D.; Fricke, C. L.; Long, S. A. T.; Landon, W. F.; and Ridge, D. L.: Preliminary Analysis of NASA Optical Data Obtained in Barium Ion Cloud Experiment of September 21, 1971. J. Geophys. Res., vol. 78, no. 25, Sept. 1, 1973, pp. 5769-5784.

2. Boehmer, Robert: A Three Station Method To Acquire Smoke Trail Position. Fourth National Conference on Aerospace Meteorology. Amer. Meteorol. Soc., 1970, pp. 151-161.

3. Beers, Yardley: Introduction to the Theory of Error. Second ed., Addison-Wesley Pub. Co., Inc., c.1957, pp. 38-43.

4. Justus, C. G.; Edwards, H. D.; and Fuller, R. N.: Analysis Techniques for Determining Mass Motions in the Upper Atmosphere From Chemical Releases. AFCRL-64-187, U.S. Air Force, Jan. 1964. (Available from DDC as AD 435 678.)

5. Hogge, John E.: Three Ballistic Camera Data Reduction Methods Applicable to Reentry Experiments. NASA TN D-4260, 1967.

6. Lloyd, K. H.: Concise Method for Photogrammetry of Objects in the Sky. WRE-TN-72, Aust. Def. Sci. Serv., Aug. 1971.

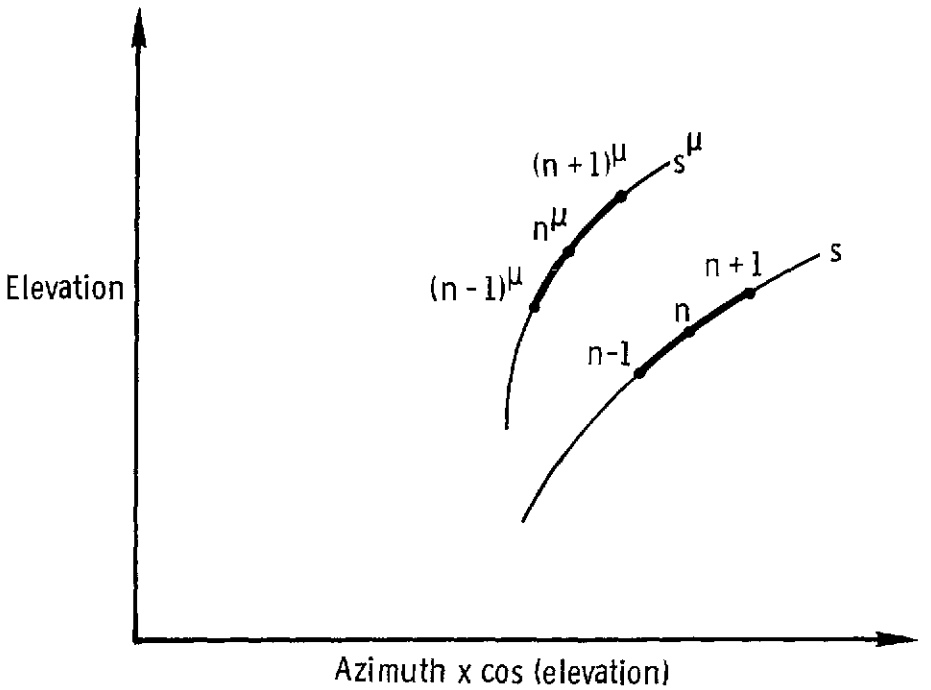

Figure 1.- From observation station μ, image trace segment $(n-1)^{\mu}$, n^{μ}, $(n+1)^{\mu}$ differing from error-free trace segment n-1, n, n+1 in location, orientation, and shape.

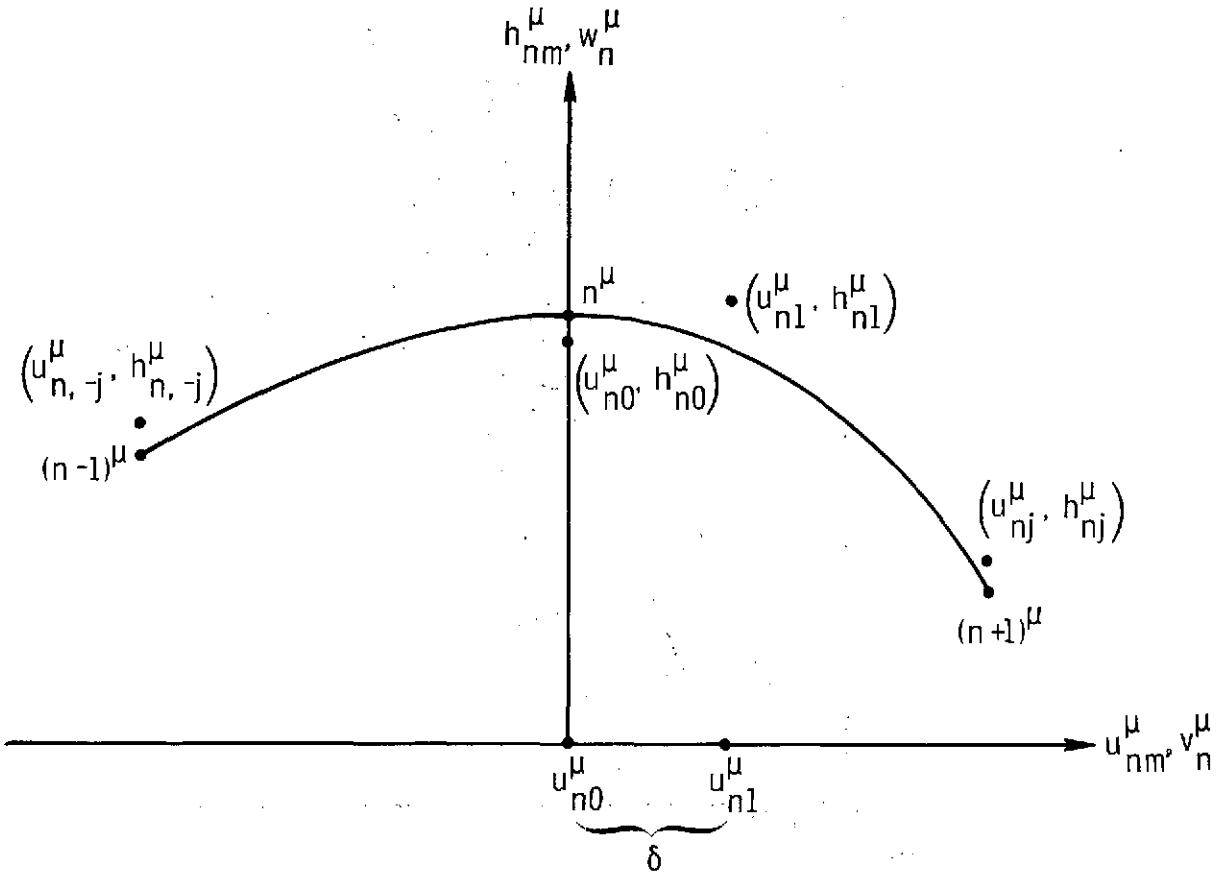

Figure 2.- Within a segment, the coordinates of the individual input data points that give rise to the second-degree curve $(n-1)^{\mu}$, n^{μ}, $(n+1)^{\mu}$.

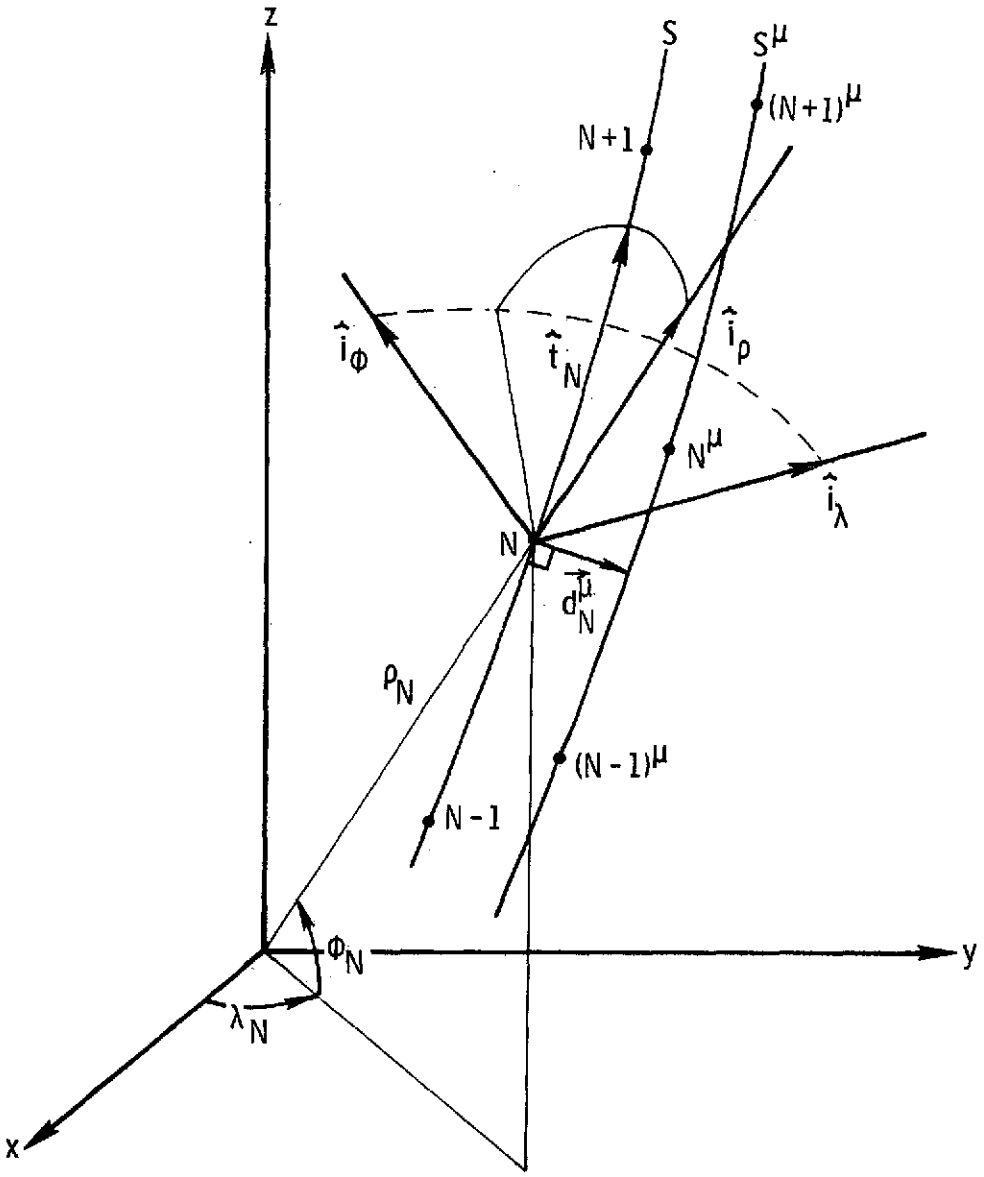

Figure 3.- In space, reference curve S, triangulation solution curve S^{μ}, and total output displacement error vector $\vec{d}_N^{\mu}$.

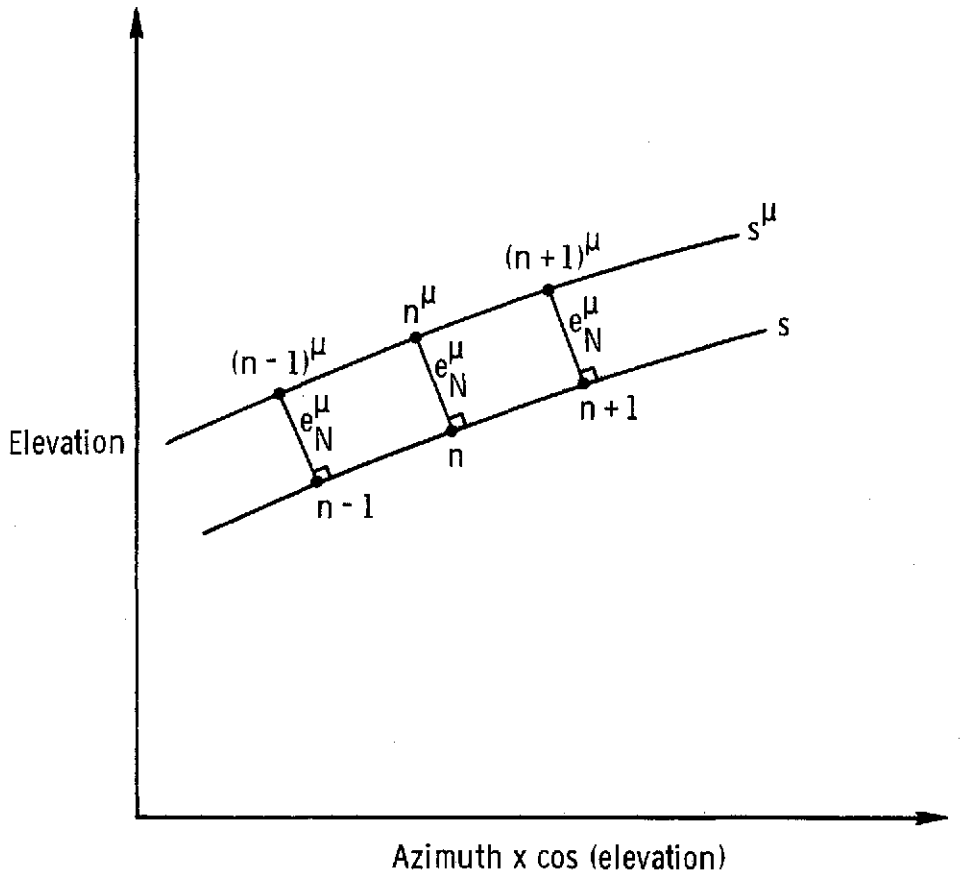

Figure 4.- From observation station μ, input displacement error e_N^{μ}.

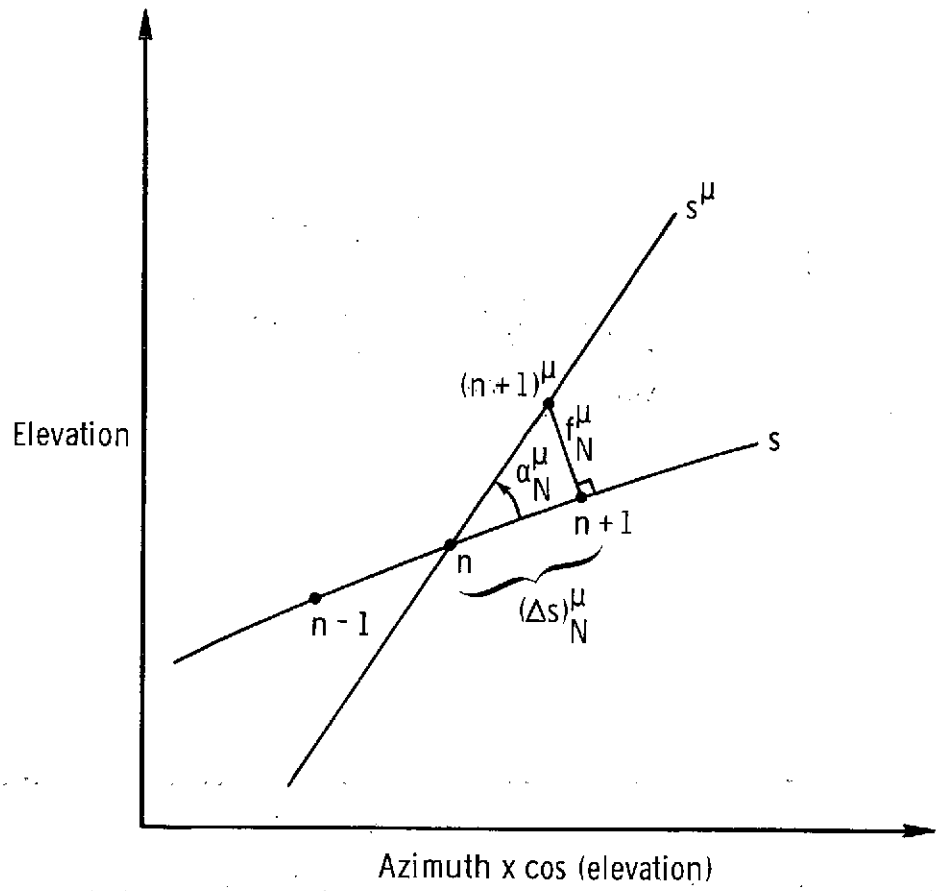

Figure 5.- From observation station μ, input slope error α_N^{μ}.

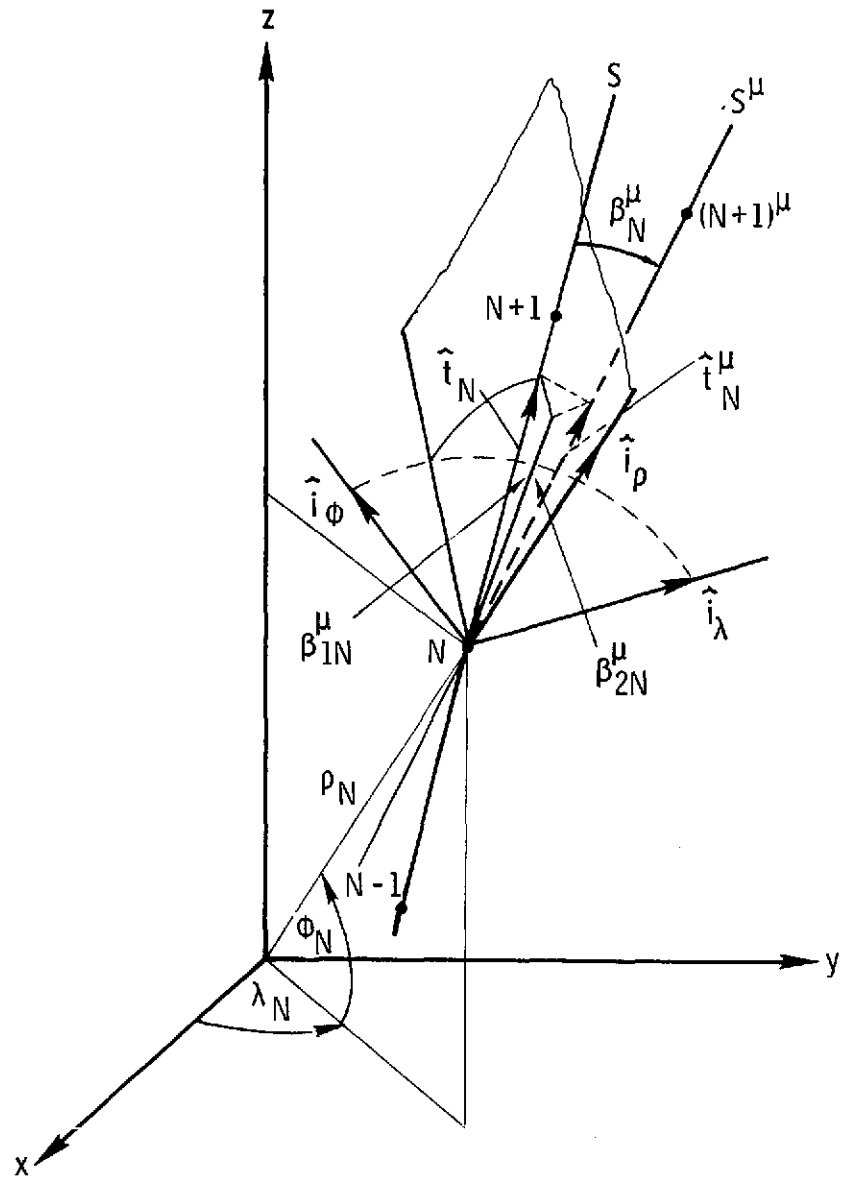

Figure 6.- In space, output slope errors β_{1N}^{μ}, β_{2N}^{μ}, and β_N^{μ}.

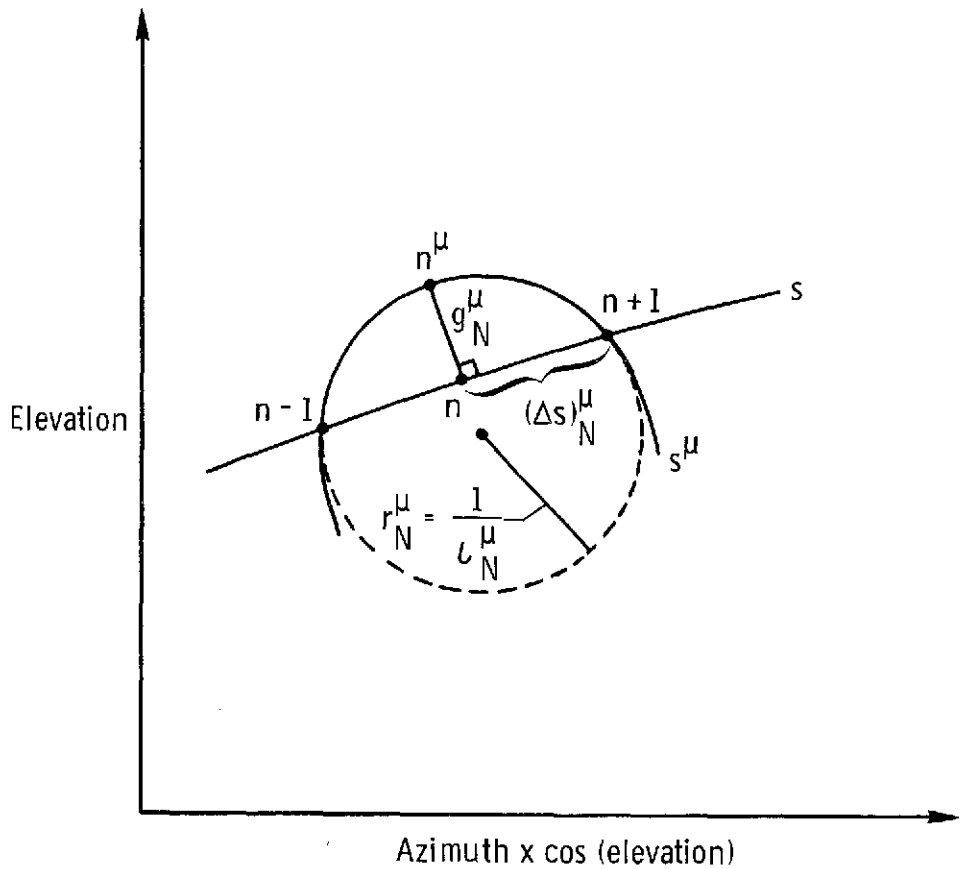

Figure 7.- From observation station μ, input curvature error ι^{μ}_{N}.

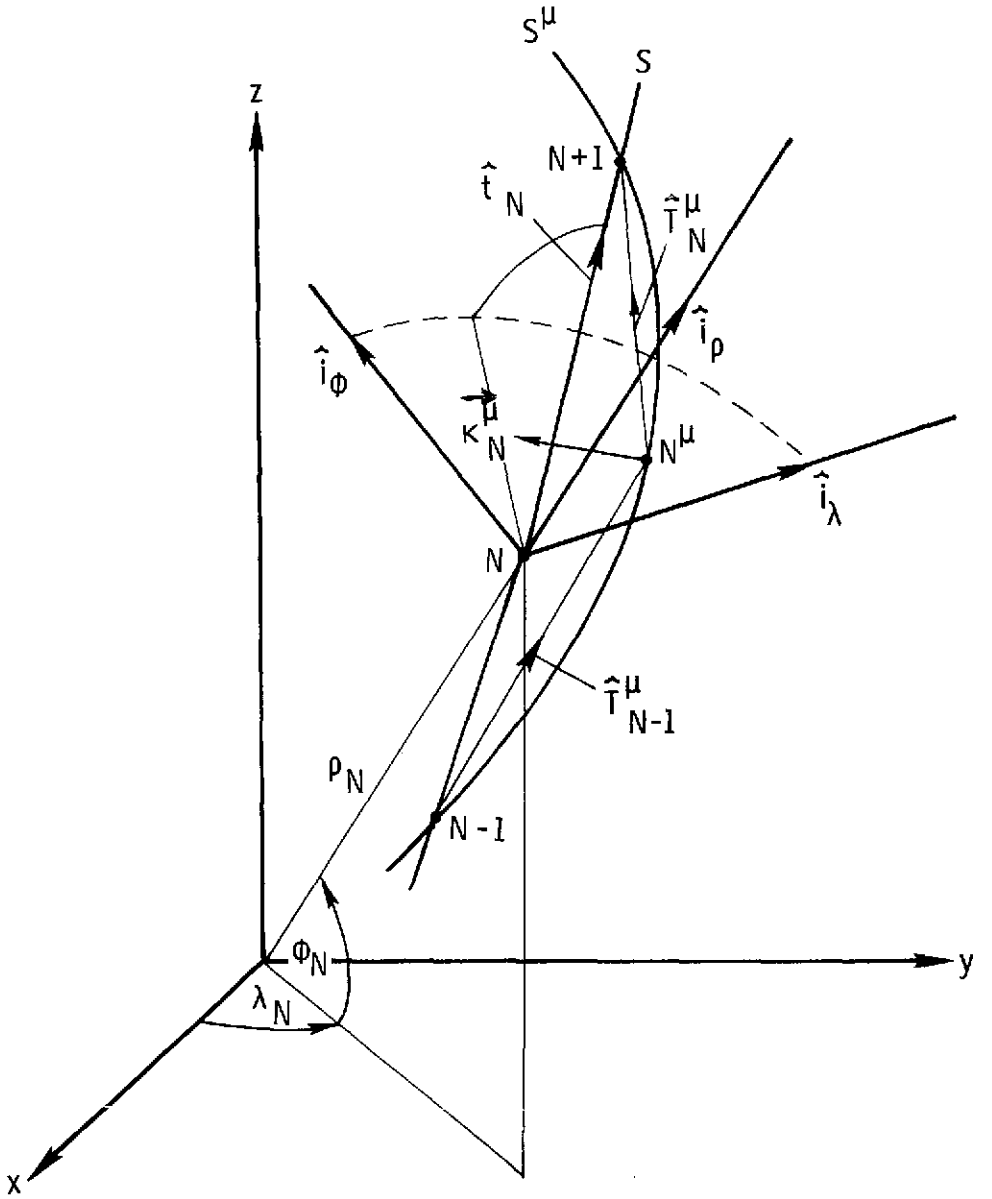

Figure 8.- In space, total output curvature error vector $\vec{\kappa}^\mu_N$.